THE JOURNAL OF PHYSICAL CHEMISTRY C

Article

pubs.acs.org/JPCC

Enhancement of Lithium Ion Mobility in Ionic Liquid Electrolytes in Presence of Additives

Anirudh Deshpande, Lahiru Kariyawasam, Prashanta Dutta, and Soumik Banerjee*

School of Mechanical and Materials Engineering Washington State University, Pullman, Washington 99164-2920, United States

Supporting Information

ABSTRACT: Ionic liquids are widely considered as potential electrolytes for lithium batteries due to their tunable electrochemical properties. In the present study, the mobility and transport characteristics of lithium ions in *N*-methyl-*N*-propylpyrrolidinium bis(trifluoromethanesulfonyl)imide ($mppy^+TFSI^-$) ionic liquids were characterized using the molecular dynamics method. Results from the simulations indicate that inclusion of organic additives such as ethylene carbonate, vinylene carbonate, and tetrahydrofuran decreases the extent of coordination of the lithium ion with the anion of the ionic liquid and hence increases its mobility and overall ionic conductivity. The mobility of lithium ions in the ionic liquid based electrolyte increases with increasing concentration of the additive. Of the additives investigated, ethylene carbonate was identified as the most effective in increasing the mobility of lithium ions, while vinylene carbonate increases the overall ionic conductivity to the greatest extent.

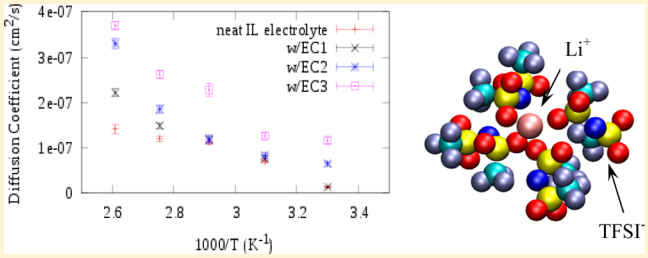

1. INTRODUCTION

Among the myriad energy-storage technologies that are currently used, rechargeable lithium ion batteries are widely used as energy sources for a range of portable electronic devices because of their relatively high specific energy storage capabilities.[1] However, the highest energy storage capacity achieved by state-of-the-art lithium ion battery is too low to meet current demands in larger applications such as in the automotive industry.[2] The limitation is due, in part, to the limited ionic conductivity of currently used organic electrolytes coupled with their volatility and electrochemical instability.[3] Commercial lithium ion batteries use organic solvents, such as ethylene carbonate or diethyl carbonates, with noncoordinating anion salts such as lithium bis(trifluoromethanesulfonyl)imide (Li^+TFSI^-) and hexafluorophosphate ($LiPF_6$).[4] The relatively high vapor pressure of these electrolytes makes them flammable, which raises safety concerns.[5] The development of efficient batteries therefore requires identification of improved electrolytes without compromising on safety standards.

Ionic liquids, which are liquid salts at room temperature, are being currently investigated as potential electrolytes due to their favorable properties such as low volatility as well as high thermal and chemical stability.[6] Unlike conventional electrolytes, ionic liquids are nonhazardous, have low vapor pressures, and are nonflammable, which make them suitable candidates for use in lithium ion batteries. For instance, *N*-methyl-*N*-propylpyrrolidinium bis(trifluoromethanesulfonyl)imide ($mppy^+TFSI^-$) ionic liquid is known to have a wide electrochemical window.[7] The $mppy^+TFSI^-$ ionic liquid doped with lithium salt has been reported to allow lithium to be recycled with a high degree of reversibility at moderate current densities. However, a major disadvantage of this ionic liquid is that the $TFSI^-$ ion produces significant charge localization, which results in strong coordination of Li^+ and $TFSI^-$ ions.[8] The anion coordinates with Li^+, which tends to form a segregation of negatively charged clusters in the isotropic and homogeneous liquid.[9] The heterogeneity is explained by the short-range interactions of the tail groups of $mppy^+$ cations and the long-range Coulombic forces between the head groups of cations and anions.[10] Alkyl groups in $mppy^+$ cations also increase the heterogeneity due to the van der Waals interactions between the alkyl chains. The negatively charged clusters reduce the mobility of lithium ions within the system[8] and therefore reduce the ionic conductivity of the lithium-doped $mppy^+TFSI^-$ ionic liquid electrolyte. In an effort to improve the transport properties in these materials, various scientific efforts have been directed to design low-viscosity ions with enhanced ionic conductivity.[11] However, synthesizing new ionic liquids with low viscosity is a complex process,[12] and an immediate solution would be to introduce small amounts of molecular additives. In particular, organic additives have the ability to improve the electrolyte by enhancing the transport properties of ions[8] as well as by improving the solid electrolyte interphase.[13] Several studies have investigated the addition of organic solvents in ionic liquids[14] to improve their properties, such as an increase in the efficiency of lithium plating and stripping[15] while maintaining the nonflammability characteristics of ionic liquids.[16]

Received: September 23, 2013
Revised: November 11, 2013
Published: November 13, 2013

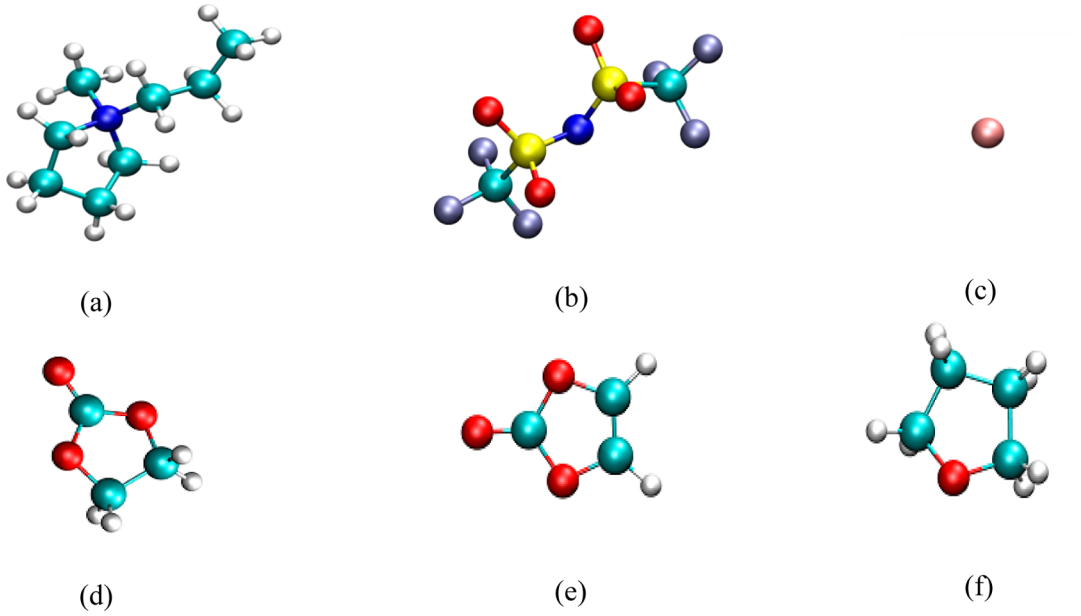

Figure 1. Molecular structures of (a) $mppy^+$, (b) $TFSI^-$, (c) Li^+, (d) ethylene carbonate, (e) tetrahydrofuran, and (f) vinylene carbonate are shown. The corresponding atoms are denoted as cyan = carbon, red = oxygen, blue = nitrogen, gray = hydrogen, ice blue = fluorine, yellow = sulfur, and pink = lithium.

Recently, Raman spectroscopy was used to show that in the presence of additives such as ethylene carbonate or vinylene carbonate the extent of coordination of Li^+ with the anion of the ionic liquid is diminished.[8] While the transport properties of ions in neat ionic liquids are well understood and have been characterized by various experimental as well as theoretical and molecular modeling studies in recent years,[17−23] the mobility of Li^+ ions in ionic liquids doped with additives has not been investigated. Molecular dynamics simulations, which directly account for interatomic interactions, are well suited to evaluate the mobility of ions within an ionic liquid doped with additives and to relate the ionic conductivity to the molecular structure of the additives and ions.[7]

In this paper, we report results from molecular dynamics simulations to understand the effects of additives on the mobility of Li^+. We have simulated $mppy^+TFSI^-$ ionic liquid doped with Li^+TFSI^- as a model system. The additives used in our study were ethylene carbonate, vinylene carbonate, and tetrahydrofuran at various concentrations (0.069, 0.13, and 0.2 mole fraction) and at different temperatures. Figure 1 illustrates all the ions and the additives that were simulated. We evaluated self-diffusion coefficients of Li^+ ions in ionic liquid in the presence of additives. In an effort to relate ion mobility to various interatomic interactions, the relative coordination of Li^+ was evaluated by obtaining radial distribution functions (RDFs) of Li^+ with respect to the anion of the ionic liquid and the additives. The corresponding coordination numbers between Li^+ and the electronegative atoms of $TFSI^-$ (nitrogen, oxygen, and fluorine) as well as the additives (oxygen) were also obtained. In an effort to relate the mobility of Li^+ to the performance of the electrolyte, we also evaluated the ionic conductivity of specific ionic liquid and additive systems in which the mobility of Li^+ is significant. A hypothesis is presented to correlate the ionic conductivity to the diffusivity of the individual components in the simulated systems. Results presented in the study provide fundamental insight into the mobility of Li^+ in ionic liquids in the presence of additives and can be used to identify electrolytes for lithium ion batteries.

2. COMPUTATIONAL METHOD

We employed molecular dynamics simulations to simulate systems comprising $mppy^+TFSI^-$ ionic liquid doped with Li^+TFSI^- salt with or without additives. *Ab initio* charge calculations were performed on a cation/anion pair with the second-order Moller−Plesset (MP2) perturbation theory using the 6-31G(d) basis set[24−31] to obtain the partial atomic charges. Table 1 provides a list of partial charges for the electronegative

Table 1. Partial Charges of Li^+ and the Electronegative Atoms of $TFSI^-$, Ethylene Carbonate, Vinylene Carbonate, and Tetrahydrofuran

atom	partial charge (in terms of electronic charge, *e*)
$N(mppy^+)$	0.4652
$N(TFSI^-)$	−0.8759
$O(TFSI^-)$	−0.6643/−0.6551
"═O" EC	−0.6250
"═O" VC	−0.6128
"−O" EC	−0.5041/−0.4802
"−O" VC	−0.3484/−0.3354
"−O" THF	−0.5189
Li^+	0.8974

atoms of $mppy^+$, $TFSI^-$, the additives, and Li^+. We used the software LAMMPS[32] for all classical molecular dynamics simulations. We employed the optimized potentials for liquid simulations (OPLS) force field[33] to describe the atomic interactions. We validated our results by comparing calculated properties, such as density and diffusion coefficient for neat ionic liquid and ionic liquid doped with Li^+TFSI^-, to experimental data. The relevant computational details and results are provided as Supporting Information. For the doped solution (IL with Li^+TFSI^-), which served as a benchmark for obtaining enhancement in diffusion coefficients and ionic

dx.doi.org/10.1021/jp409498w | J. Phys. Chem. C 2013, 117, 25343−25351

conductivities for systems with additives, a mixture of 0.25 mole fraction Li^+TFSI^- with 0.75 mole fraction $mppy^+TFSI^-$ was simulated. Systems with the additives comprised of ethylene carbonate, vinylene carbonate, and tetrahydrofuran with mole fractions of 0.069, 0.13, and 0.2 added to the doped ionic liquid system. Greater mole fractions will increase the vapor pressure of the mixed systems and were hence not considered in the present study.

An *NPT* ensemble, where the number of particles (N), pressure (P), and temperature (T) are fixed, was used to equilibrate each system at atmospheric pressure and temperatures of 303, 323, 343, 363, and 383 K. A Nosé−Hoover barostat[34−37] and thermostat[38−42] were utilized to control the temperature and pressure. Production runs of *NVT* ensembles, where the volume (V) is fixed, were carried out for at least 80 ns at constant temperatures. The equations of motion were integrated with a time step of 1 fs (fs). The cutoff distances for van der Waals and Coulombic interactions were 1.5 nm. Long-range electrostatic interactions were computed using the particle−particle−particle mesh (PPPM) method.[43−51]

3. RESULTS AND DISCUSSION

In an effort to evaluate the effect of additives on the mobility of Li^+ ions in ionic liquids, we calculated the diffusion coefficients of Li^+ in ionic liquid based electrolytes, comprising neat ionic liquid doped with Li^+TFSI^- salt, with additives ethylene carbonate, vinylene carbonate, and tetrahydrofuran, at concentrations of 0.069, 0.13, and 0.2 by mole fraction. For the sake of convenience, we designate systems with varying concentrations of additives with abbreviated nomenclature. For instance, systems with additive mole fraction of 0.069 are denoted as EC1/VC1/THF1, mole fraction of 0.13 as EC2/VC2/THF2, and mole fraction of 0.2 as EC3/VC3/THF3. Ionic liquid with Li^+TFSI^- without any additive is designated as neat IL electrolyte. As a reference, the diffusion coefficient of Li^+ was also calculated in the neat IL electrolyte without additives.

The self-diffusion coefficients, D, were calculated from mean-squared displacements based on Einstein's relation, which is given by[52,53]

$$D = \lim_{t\to\infty} \frac{1}{6Nt} \left\langle \sum_{j=1}^{N} [r_j(t) - r_j(0)]^2 \right\rangle \quad (1)$$

where $\langle\ \rangle$ designates ensemble average, t is the time interval, N is the number of ions, and $r_j(t)$ denotes position of ionic species j at time t. Linear regression analysis was used to obtain the slope from the mean-squared displacements at various time intervals. Relevant error bars were calculated and are supplied in the plots. The plots in Figure 2 show values of diffusion coefficients obtained vs $1000/T$, with T being the temperature ranging between 303 and 383 K in increments of 20 K. The results for systems comprising ethylene carbonate, vinylene carbonate, and tetrahydrofuran additives are shown in Figures 2a, 2b, and 2c, respectively.

It is observed from Figure 2 that, in general, the diffusion coefficient of Li^+ increases with the inclusion of additives. Also, from Figure 2, we notice an increase in the diffusion coefficient of Li^+ with increase in concentration of additives. The average increase in diffusion coefficient for different additives and concentrations, compared to neat IL electrolyte, is given in Table 2. As seen in Table 2, EC1/EC2/EC3 enhances the diffusion coefficient on an average by 18.7%/120.95%/248.95% over the range of 303−383 K, as compared to 51.95%/87.65%/100.62% for VC1/VC2/VC3 and 37.41%/86.87%/97.66% for THF1/THF2/THF3, respectively. The underlying cause for the reduced mobility of Li^+ in neat IL electrolyte is the coordination of Li^+ with IL anions to form charged clusters. Therefore, the enhancement in diffusion coefficient in the presence of additives can be understood by studying the nature of association of Li^+ with other ions/atoms in the system. To quantify such association and the resulting increase in diffusion coefficient, we obtained the RDF of Li^+ with respect to the electronegative $TFSI^-$ anions, as shown in Figure 1b, and various atoms of the additives. The RDF, $g_{ab}(r)$, between two atoms a and b, is given by[52,53]

$$g_{ab}(r) = \frac{dn_{ab}(r)}{4\pi r^2 dr \rho_a} \quad (2)$$

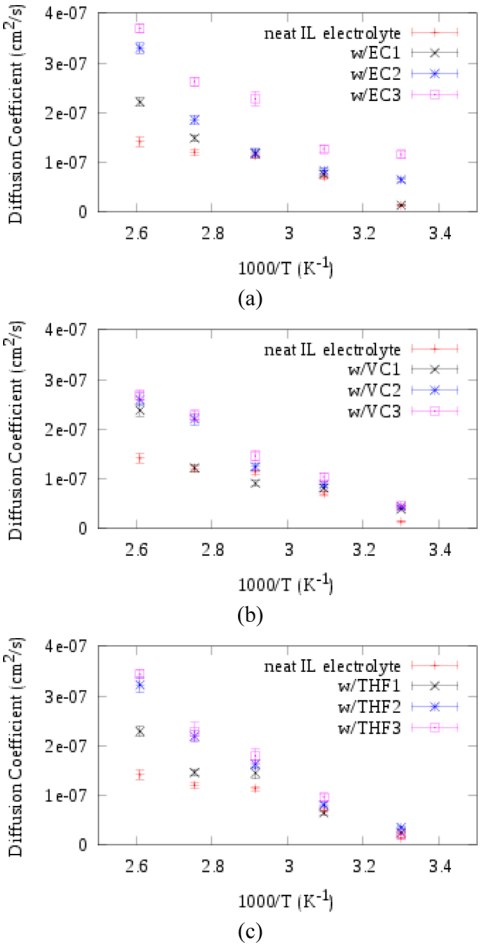

Figure 2. Self-diffusion coefficient of lithium ion, D_{Li^+}, as a function of $1000/T$ (K^{-1}) is evaluated for the neat IL electrolyte system and compared with (a) D_{Li^+} for ethylene carbonate, (b) D_{Li^+} for vinylene carbonate, and (c) D_{Li^+} for tetrahydrofuran.

Table 2. Percentage Increase in Diffusion Coefficient of Li^+ for All the Systems with Additives

additive concn (mole fraction)	ethylene carbonate (%)	vinylene carbonate (%)	tetrahydrofuran (%)
0.069	18.75	51.95	37.41
0.13	120.95	87.65	86.87
0.2	248.95	100.62	97.66

dx.doi.org/10.1021/jp409498w | J. Phys. Chem. C 2013, 117, 25343−25351

where $dn_{ab}(r)$ is the average number of b atoms within a spherical shell of radius r and thickness dr enclosing an a atom placed at $r = 0$, and ρ_a is the number density of atom a in the simulated ionic liquid system. The $TFSI^-$ ion, as shown in Figure 1b, is comprised of nitrogen, oxygen, sulfur, and fluorine, with nitrogen being negatively charged. The electronegativity of these atoms is indicated by their partial charges shown in Table 1. The oxygen atom of $TFSI^-$, designated as O($TFSI^-$), has a partial negative charge of $-0.6551e$, which is comparable with the electronegative oxygen of the additives. However, the O($TFSI^-$) are surrounded by electropositive sulfur ($+1.317e$) which makes it sterically difficult for the Li^+ ions to coordinate with the O($TFSI^-$). The nitrogen of $mppy^+$ also has a partial positive charge (+0.4652), which will repel the Li^+. Thus, Li^+ would have a natural tendency to coordinate with the nitrogen of $TFSI^-$ [N($TFSI^-$)], which is the most electronegative atom in $TFSI^-$. Therefore, in our analysis, we obtained RDFs of Li^+ with respect to N($TFSI^-$). In an effort to investigate the increase in diffusion coefficient with increase in concentration of additive, we first evaluated the RDFs for Li^+ with respect to N($TFSI^-$) for neat IL electrolyte, EC1, EC2, and EC3 at a reference temperature of 323 K, as shown in Figure 3a. From

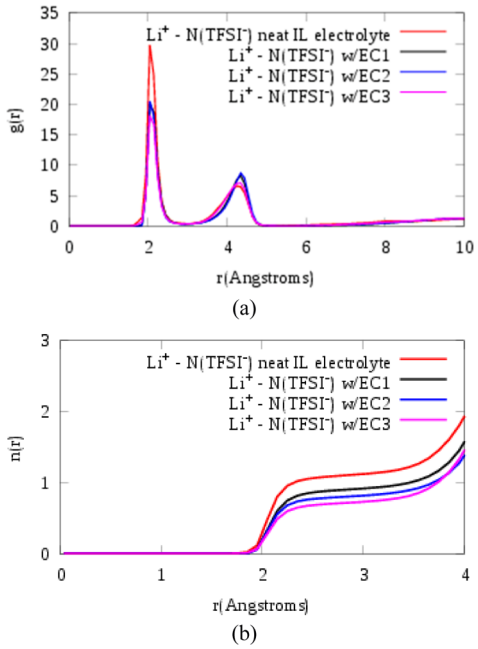

Figure 3. (a) Radial distribution function of Li^+ with respect to N($TFSI^-$) for neat IL electrolyte, EC1, EC2, and EC3 at 323 K. (b) Coordination number of Li^+ with N($TFSI^-$) in neat IL electrolyte, EC1, EC2, and EC3 at 323 K.

the figure, we notice that the observed peak of $g(r)$ at 2 Å for neat IL electrolyte (~30) is greater than EC1 (~20), EC2 (~19), and EC3 (~18), suggesting that the probability of finding a N($TFSI^-$) surrounding a Li^+ in neat IL electrolyte is higher than that in IL with additives. To further quantify our result, we obtained the coordination number of Li^+ surrounded by N($TFSI^-$). The coordination number $n(r)$ between two atoms is obtained by integrating the weighted RDF between atoms and is given by[52,53]

$$n(r) = 4\pi\rho \int_0^r x^2 g_{ab}(x)\, dx \qquad (3)$$

As seen in Figure 3b, the coordination number for Li^+ and N($TFSI^-$) at 3.5 Å is greater for neat IL electrolyte (~1.1) followed by EC1 (~0.9), EC2 (~0.8), and EC3 (~0.6). This trend suggests that fewer N($TFSI^-$) are coordinated with Li^+ for EC3, followed by EC2, EC1, and neat IL electrolyte. These results are directly correlated with the Li^+ diffusion coefficients. The diffusion coefficients for neat IL electrolyte, EC1, EC2, and EC3 at 323 K were found to be 6.98×10^{-7}, 7.64×10^{-7}, 8.29×10^{-7}, and 1.27×10^{-7} cm^2/s, respectively.

Similarly, we also determined the coordination number of Li^+ and N($TFSI^-$) and diffusion coefficient for vinylene carbonate and tetrahydrofuran, at the same reference temperature of 323 K. For vinylene carbonate, the coordination number between Li^+ and N($TFSI^-$) at 3.5 Å was found to be ~1.2 for VC1, ~1.0 for VC2, and ~0.6 for VC3, as shown in Table 3. The

Table 3. Coordination Numbers of Li^+ with N($TFSI^-$) for Systems Comprising Neat Ionic Liquid Electrolyte as Well as Systems with Additives at Various Concentrations

additive concentration	ethylene carbonate	vinylene carbonate	tetrahydrofuran
neat IL electrolyte	1.1	1.1	1.1
0.069 mole fraction	0.9	1.2	1.4
0.13 mole fraction	0.8	1.0	1.1
0.2 mole fraction	0.6	0.6	0.9

corresponding diffusion coefficients obtained were 8.11×10^{-8} cm^2/s for VC1, 8.78×10^{-8} cm^2/s for VC2, and 1.03×10^{-7} cm^2/s for VC3. A similar trend was also observed in the case of IL with tetrahydrofuran. We found that the coordination between Li^+ and N($TFSI^-$) was ~1.4 for THF1, ~1.1 for THF2, and ~0.9 for THF3, and the diffusion coefficients obtained were 6.37×10^{-8} cm^2/s for THF1, 8.04×10^{-8} cm^2/s for THF2, and 9.61×10^{-8} cm^2/s for THF3. We observed that for VC1 and THF1 there is a slight increase in the coordination between Li^+ and N($TFSI^-$), compared to neat IL electrolyte, which decreases at higher concentrations of additives. In order to analyze this trend, we calculated the coordination number of Li^+ with respect to the oxygen atom of $TFSI^-$ [denoted as O($TFSI^-$)] for various systems. The oxygen atom was chosen because it is the second most electronegative atom in $TFSI^-$, as shown in Table 1. Our results indicate that the coordination between Li^+ and O($TFSI^-$) decreases from ~4 in neat IL electrolyte to ~2.5 in VC1. In the case of THF1, Li^+–O($TFSI^-$) coordination remains almost the same as that for neat IL electrolyte for shorter length scales up to 3.5 Å. However, beyond 4 Å, the coordination number decreases from ~7 in neat IL electrolyte to ~6 in THF1. The relatively feeble effect of tetrahydrofuran in reducing the coordination between Li^+ and O($TFSI^-$) at low concentrations (THF1) is due to the significantly lower partial charge of oxygen of tetrahydrofuran compared to that of vinylene carbonate, as seen in Table 1. From this analysis, it can be concluded that while vinylene carbonate and tetrahydrofuran are not effective in reducing coordination of Li^+ with N($TFSI^-$) at low concentrations, they do help in reducing the overall coordination between Li^+ and the entire $TFSI^-$, particularly with the oxygen atom. This reduced coordination results in increase in values of diffusion coefficients. Additionally, since vinylene carbonate is more effective in reducing coordination with O($TFSI^-$) at low concentrations, VC1 is a better additive system than THF1. To understand this trend in further details, it is important to

dx.doi.org/10.1021/jp409498w | J. Phys. Chem. C 2013, 117, 25343−25351

determine how the concentration of additive affects the interaction of Li^+ with the additives inside the system.

In an effort to determine the association of Li^+ with the additive, we first need to identify the most electronegative atoms of the additive. As seen previously for $TFSI^-$, the partial charges of the atoms of the additive help us to identify the most electronegative atom. From Table 1, it can be seen that for tetrahydrofuran the single oxygen atom present in the ring is the most electronegative atom [denoted as O(−THF)], with a partial charge of −0.5189*e*. But for ethylene and vinylene carbonate, there are three oxygen atoms present in the ion. The most electronegative atom is the double-bonded oxygen, with a partial charge of −0.6250*e* and −0.6128*e* for ethylene and vinylene carbonate, respectively [denoted as O(═EC) and O(═VC)]. We therefore evaluated the RDF between Li^+ and the double-bonded O atom of ethylene carbonate additive for all concentrations as a reference case. Figure 4 shows the

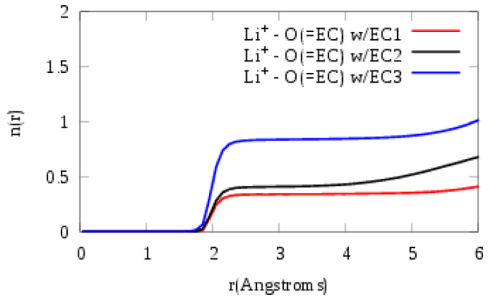

Figure 4. Coordination numbers of Li^+ with double-bonded oxygen of ethylene carbonate at all concentrations at 323 K.

coordination of Li^+ with the double-bonded oxygen of ethylene carbonate, for EC1, EC2, and EC3, at the same reference temperature of 323 K. The coordination between Li^+ and O(═EC) for EC3 is the highest (∼0.8), followed by EC2 (∼0.4) and EC1 (∼0.3). Since the increase in concentration of additive leads to favorable association of Li^+ with the additives in comparison to that with the $TFSI^-$ anion, we hypothesize that the mobility and hence diffusion coefficient of Li^+ will increase with additive concentration, which was also seen in Figure 2. It can be concluded from these plots that in presence of an additive, such as ethylene carbonate, the Li^+ ions preferentially coordinate with the electronegative oxygen of ethylene carbonate rather than the electronegative nitrogen of $TFSI^-$ and forms a smaller cluster. Therefore, the mobility of Li^+ ion is enhanced in the presence of additives.

The second step of our analysis focused on understanding the variation of diffusion coefficient for each of the additives at a fixed concentration. As seen previously in Figure 2 and Table 2, ethylene carbonate has a greater impact on increasing the diffusion coefficient of Li^+ as compared to vinylene carbonate and tetrahydrofuran. This higher percentage increase in diffusion coefficient for EC3 can be explained by analyzing the coordination of Li^+ with N($TFSI^-$) for each of the additives at the same concentration. We evaluated the coordination of Li^+ with N($TFSI^-$) for a reference concentration of 0.2 mole fraction (EC3, VC3, and THF3) at a reference temperature of 323 K, as shown in Figure 5a. The coordination of Li^+ with N($TFSI^-$) is the least for EC3 (∼0.7), followed by VC3 (∼0.9) and THF3 (∼1.0). These values follow the same trend as the diffusion coefficients obtained: 1.27×10^{-7} cm^2/s for EC3, 1.03×10^{-7} cm^2/s for VC3, and 9.61×10^{-8} cm^2/s for THF3. To

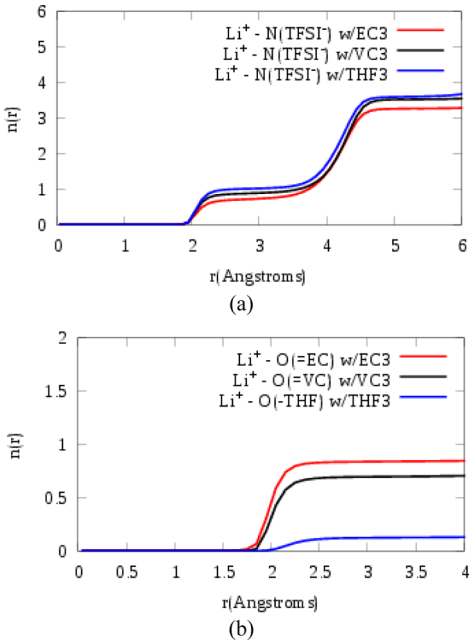

Figure 5. (a) Coordination number of Li^+ with respect to N($TFSI^-$) in EC3, VC3, and THF3 at 323 K. (b) Coordination of Li^+ with single-bonded oxygen of ethylene carbonate, vinylene carbonate, and tetrahydrofuran in EC3, VC3, and THF3, respectively, at 323 K.

obtain greater insight into the mechanism that leads to increase in diffusion coefficient of Li^+, we obtained the coordination of Li^+ with the most electronegative atom of the additive that were identified earlier from Table 1. From Figure 5b, we find that Li^+ preferentially coordinates with the double-bonded oxygen of ethylene carbonate and vinylene carbonate and the single-bonded oxygen of tetrahydrofuran, which helps in reducing the Li^+ N($TFSI^-$) coordination. The low coordination number for Li^+ and single-bonded oxygen of THF3 [O(−THF)] (∼0.1) as compared to Li^+ and O(═VC) (∼0.7) in VC3 and Li^+ and O(═EC) (∼0.8) in EC3 correlates with the low diffusion coefficient for IL with THF3 compared to IL with VC3 and IL with EC3.

To determine the comparative effect of different additives on the mobility of Li^+, we analyzed respective molecular structures (shown in Figure 1) and partial charges of the additive atoms, provided in Table 1, that coordinate with Li^+. For ethylene carbonate (shown in Figure 1d), the double-bonded oxygen has a partial charge of −0.62507*e* whereas the single-bonded oxygen has a partial charge of −0.50411*e*. The high electronegativity of these oxygen atoms helps reducing the coordination between Li^+ and N($TFSI^-$). Similar oxygen atoms are also present in the molecular structure of vinylene carbonate (shown in Figure 1e). However, the partial charges of the double- and single-bonded oxygen in vinylene carbonate (−0.6128*e* and −0.3484*e*) are slightly lower than those of ethylene carbonate. The presence of the two extra hydrogen atoms attached to the carbon atoms in the ring in case of ethylene carbonate induce a negative charge on the surrounding single-bonded oxygen atoms. However, the partial negative charge on the single-bonded oxygen atoms of vinylene carbonate is lower because of two fewer hydrogen atoms on the carbon atoms, and the electronegative carbon atoms attached by a double bond. Lower electronegativity of oxygen atoms in vinylene carbonate than ethylene carbonate causes a stronger Li^+ N($TFSI^-$) coordination for IL with vinylene

dx.doi.org/10.1021/jp409498w | J. Phys. Chem. C 2013, 117, 25343−25351

carbonate as compared to ethylene carbonate. As shown in Figure 1f, tetrahydrofuran has only one single-bonded oxygen atom. However, the partial charge for this oxygen ($-0.5189e$), provided in Table 2, is greater in magnitude compared to single-bonded oxygen of vinylene carbonate ($-0.3484e$) but comparable with the single-bonded oxygen of ethylene carbonate ($-0.5041e$). While this single oxygen atom, due to its high electronegativity, is responsible for reducing the coordination between Li^+ and $N(TFSI^-)$, it is less effective than that of ethylene carbonate or vinylene carbonate.

To better understand the observed effect of temperature on self-diffusion coefficients, as shown in Figure 2, we calculated the RDF between Li^+ and $N(TFSI^-)$ for a reference case of EC3 at two separate temperatures of 303 and 383 K (Figure 5). As seen in Figure 6a, the first peak of $g(r)$ at 2 Å for EC3 at 303

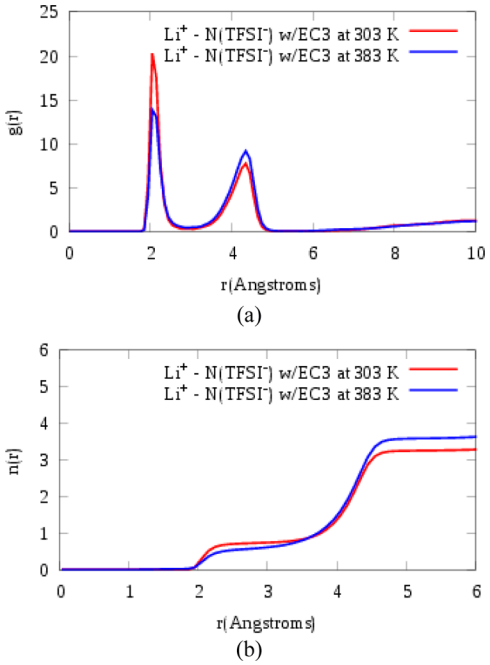

Figure 6. (a) Radial distribution function of Li^+ with respect to $N(TFSI^-)$ in EC3 at 303 and 383 K and (b) corresponding coordination number of Li^+ and $N(TFSI^-)$ in EC3 evaluated at 303 and 383 K.

K (~20) is higher than that at 383 K (~12.5). Further, on the basis of coordination numbers presented in Figure 6b, we conclude that fewer $N(TFSI^-)$ ions are coordinated with Li^+ at 383 K (~0.5) than at 303 K (~0.75) at distances corresponding to the first peak in radial distribution function. The coordination number, however, is greater at 383 K as compared to 303 K, at a distance of 4.5 Å corresponding to the second peak in radial distribution function. Greater coordination between Li^+ and $N(TFSI^-)$ for longer distances, at higher temperatures, can be attributed to the structural relaxation of the Li^+TFSI^- cluster at higher temperatures. For an identical system, $N(TFSI^-)$ moves further away from the Li^+, causing a reduction of coordination at shorter distances and a corresponding increase at larger distances. In addition to the formation of a less compact cluster with $TFSI^-$ anion, the diffusion coefficient of Li^+ increases at greater temperature. At 303 K for EC3 the diffusion coefficient of Li^+ is 1.15×10^{-7} cm^2/s, whereas at 383 K, it is 3.7×10^{-7} cm^2/s. This increase in diffusion coefficient with increase in temperature, which is widely known,[54] can be explained by the fact that at higher temperatures Li^+ ions possess greater average kinetic energy, which enhances the mobility of Li^+ ions in the system. This results in diminished coordination between Li^+ and $N(TFSI^-)$ at higher temperature compared to that at low temperatures, which increases the diffusion coefficients, as seen in Figure 2.

In an effort to compare the efficacy of various additives in enhancing the overall performance of the electrolyte systems, we calculated the ionic conductivity, λ, in systems with IL and additive by analyzing the molecular trajectory based on the relation[52,53]

$$\lambda = \lim_{t\to\infty} \lambda(t) = \lim_{t\to\infty} \frac{e^2}{6tVk_BT} \sum_{ij}^{N} Z_iZ_j\langle[r_i(t) - r_i(0)][r_j(t) - r_j(0)]\rangle \quad (4)$$

where N is the number of types of ionic species in the system, e is the electronic charge, V is the volume of the simulation box, z_i and z_j are the charges on ions of type i and j, and r_i is the displacement of ion i at time t. To compare the overall ionic conductivity of systems with different additives, we selected a reference concentration of 0.2 by mole fraction for each additive (EC3, VC3, and THF3) at 323 K and calculated the ionic conductivity for each of the three systems. As a reference for comparison of the effectiveness of additives, we calculated the ionic conductivity of neat IL electrolyte at 323 K.

The calculated value of overall ionic conductivity is the highest for VC3 (3.67×10^{-3} S/cm), followed by EC3 (3.31×10^{-3} S/cm) and THF3 (3.15×10^{-3} S/cm). For neat IL electrolyte, the overall ionic conductivity is 2.61×10^{-3} S/cm. We saw an increase of 40.61% in the overall ionic conductivity for VC3, 26.81% for EC3, and 20.69% for THF3 compared to neat IL electrolyte. Therefore, at the highest concentrations of additives that were simulated, vinylene carbonate was the most effective additive in enhancing the overall ionic conductivity of the electrolyte while tetrahydrofuran was the least effective. It is interesting to note that while the diffusion coefficient of Li^+ in EC3 is greater than that in VC3, the latter system has a greater overall ionic conductivity. To further explain this trend, we analyzed the correlation between the overall ionic conductivity and the diffusion coefficients of the individual ions in the simulated systems, namely Li^+, $mppy^+$, and $TFSI^-$. As seen from eq 4, the overall ionic conductivity depends on the correlated displacements of all the charged species in the system (Li^+, $mppy^+$, $TFSI^-$), whereas the diffusion coefficient of Li^+, as calculated from eq 1, depends on the displacements of solely Li^+ ions. The degree of uncorrelated ion motion (α), defined as the ratio of the total ionic conductivity (λ) to the ionic conductivity due to self-diffusion only (λ_{uncorr}),[7] is a widely defined parameter for evaluating the contribution of correlated ion motion to the ionic conductivity. Mathematically, α is defined as

$$\alpha = \frac{\lambda}{\lambda_{uncorr}} \quad (5)$$

where λ_{uncorr} is given by

dx.doi.org/10.1021/jp409498w | J. Phys. Chem. C 2013, 117, 25343−25351

$$\lambda_{\text{uncorr}} = \frac{e^2}{6tVk_BT}(n_{Li^+}D_{Li^+} + n_{mppy^+}D_{mppy^+} + n_{TFSI^-}D_{TFSI^-}) = \frac{e^2}{6tVk_BT}\sum_i^N Z_i^2\langle[r_i(t) - r_i(0)]^2\rangle \quad (6)$$

Here, n_i denotes the number of ions of type i. For $\alpha = 1$, the motion of the ions is said to be completely uncorrelated and $0 \leq \alpha < 1$ implies motion due to correlated movement of ions in the system. Equation 6 demonstrates that the ionic conductivity due to uncorrelated motion depends directly on the diffusion coefficients of the charged species in the system. The partial ionic conductivity of Li^+ in a system is defined as a function of the overall ionic conductivity by the equation

$$\lambda_{Li^+} = \frac{n_{Li^+}D_{Li^+}}{n_{Li^+}D_{Li^+} + n_{mppy^+}D_{mppy^+} + n_{TFSI^-}D_{TFSI^-}}\lambda \quad (7)$$

Equation 7, however, is valid only for systems with predominantly uncorrelated motion of ions, i.e., in systems where $\alpha \geq 0.5$. Also, the partial ionic conductivity of Li^+ (λ_{Li^+}) calculated from eq 7 is approximate, and cannot be considered as the exact value, unless the motion of ions is almost completely uncorrelated, i.e. $\alpha \sim 1$, which is possible only in dilute solutions. To determine the degree of uncorrelated motion in the simulated systems with additives and to compare the overall ionic conductivity for various systems, we evaluated the values of α for EC3, VC3, and THF3 at 323 K. Values of α, provided in Table 4, were found to be 0.38 for EC3, 0.39 for VC3, 0.43 for THF3, and 0.49 for neat IL electrolyte. The low value of α for EC3 signifies that the correlation between ions in the system is greater as compared to VC3, THF3, and neat IL electrolyte. Note that we cannot compare our systems by comparing the ionic conductivity of Li^+ using eq 7 as the values obtained for α are much less than 1. We can, however, compare the uncorrelated motion of ions in different systems. As mentioned earlier, the ionic conductivity due to uncorrelated motion depends on the diffusion coefficients of the ions, which, in our case, are D_{Li^+}, D_{mppy^+}, and D_{TFSI^-} as shown in eq 6. The calculated values of diffusion coefficient of $TFSI^-$ are 5.41×10^{-8} cm^2/s for EC3, 6.72×10^{-8} cm^2/s for VC3, 4.48×10^{-8} cm^2/s for THF3, and 2.28×10^{-8} cm^2/s for neat IL electrolyte. As observed earlier, the diffusion coefficient of Li^+ is greater for EC3 (1.27×10^{-7} cm^2/s) than VC3 (1.03×10^{-7} cm^2/s), but the same is not true for the diffusion coefficient of $TFSI^-$, which is the primary component in the system in terms of concentration. Our calculations also show that the diffusion coefficient of $mppy^+$ in case of EC3 (5.23×10^{-8} cm^2/s) is comparable to the diffusion coefficient of $mppy^+$ in VC3 (5.18×10^{-8} cm^2/s). Since the concentration of Li^+ in the electrolyte is much lower than that of $TFSI^-$ anion, the greater diffusion coefficient of $TFSI^-$ in the case of VC3, as compared to EC3, leads to enhanced overall ionic conductivity of the former system due to uncorrelated motion. The degree of uncorrelated ion motion, α, being nearly identical in EC3 and VC3, the total ionic conductivity of VC3 is therefore greater than that of EC3. Overall, the results for degree of uncorrelated motion and diffusion coefficients of individual components indicate that while VC10 enhances overall ionic conductivity to the greatest extent, EC3 is the most effective electrolyte for lithium batteries based on the enhanced mobility of lithium ions.

Table 4. Values of the Degree of Uncorrelated Ion Motion, α, and Ionic Conductivity, λ (S/cm), for Different Systems

species	α	λ (S/cm)
neat IL electrolyte	0.49	2.61×10^{-3}
EC3	0.38	3.31×10^{-3}
VC3	0.39	3.67×10^{-3}
THF3	0.43	3.15×10^{-3}

4. CONCLUSIONS

Results from our molecular dynamics simulations show that the transport properties, such as self-diffusion coefficient of Li^+ ions and ionic conductivities of $mppy^+TFSI^-$ based ionic liquids doped with lithium salt, are enhanced by the addition of neutral organic additives. The extent of increase in transport properties is greater for greater concentrations of the additives and at higher temperatures. We calculated RDFs and coordination numbers of Li^+ with respect to electronegative atomic sites in the ions and additives in an effort to relate the association of Li^+ with various chemical species to their resulting mobility. Our results demonstrate that the electrostatic interactions of Li^+ with various atoms of the anion and additives play an important role in enhancing the transport properties. The partial negative charges on the oxygen atoms of the simulated additives (ethylene carbonate, vinylene carbonate, and tetrahydrofuran) help in reducing the coordination of Li^+ ions with $N(TFSI^-)$ in $mppy^+TFSI^-$IL and thus reduce the extent of cluster formation. The additives are more effective at relatively high concentrations and temperatures due to greater effectiveness in reducing such coordination. Of the additives simulated in the present study, ethylene carbonate, due to its highly electronegative oxygen, is the most effective in reducing the $Li^+-N(TFSI^-)$ coordination and hence in improving the transport properties of Li^+. At a concentration of 0.2 mole fraction, it enhances the diffusion coefficient of Li^+ by 248.95% when compared to that of neat IL electrolytes. However, the overall ionic conductivity, which depends on the correlated and uncorrelated motion of all ions in the system, is enhanced to a greater extent (up to 40.61%) in the presence of vinylene carbonate than by adding ethylene carbonate (up to 26.81%) to the neat IL electrolyte. The contribution of uncorrelated ion motion to the overall ionic conductivity in the simulated systems was determined based on evaluation of degree of uncorrelated motion. Our results indicate that the greater overall ionic conductivity of VC3 than that of EC3 is due to the greater diffusivity of $TFSI^-$ in the former system. Overall, we conclude that ILs doped with small amounts of organic additives are effective in improving the transport properties of Li^+ ions in ILs, which might facilitate their use as electrolytes of commercial Li^+ ion batteries. Of all systems that were simulated, ethylene carbonate added at a mole fraction of 0.2 enhances the mobility of lithium ions to the greatest extent and therefore is a better additive than vinylene carbonate and tetrahydrofuran.

■ ASSOCIATED CONTENT

Supporting Information

Description of the validation of the force field used for the molecular dynamics simulations; neat IL and neat IL electrolyte simulated at different temperatures; densities of various simulated systems calculated and compared with experimental results of Nicotera et al;[6] radial distribution functions of oxygen and nitrogen atoms of $TFSI^-$ calculated with respect to the nitrogen atom of $mppy^+$; results showing good agreement with

dx.doi.org/10.1021/jp409498w | J. Phys. Chem. C 2013, 117, 25343−25351

the data reported by Borodin et al.[7] and Bayley et al;[55] diffusion coefficient of hydrogen atoms of $mppy^+$ obtained using Einstein's relation and matching well with experimental results reported by Nicotera et al.[6] This material is available free of charge via the Internet at http://pubs.acs.org.

AUTHOR INFORMATION

Corresponding Author

*Tel +1 509 3350294; e-mail soumik.banerjee@wsu.edu (S.B.).

Notes

The authors declare no competing financial interest.

ACKNOWLEDGMENTS

The authors acknowledge fruitful discussions with Dr. Zhengcheng Zhang at Argonne National Laboratory. The authors acknowledge funding from the Joint Center for Aerospace Technology Innovation (JCATI) sponsored by the State of Washington.

REFERENCES

(1) Lu, Y. C.; Gallant, B. M.; Kwabi, D. G.; Harding, J. R.; Mitchell, R. R.; Whittingham, M. S.; Shao-Horn, Y. Lithium-Oxygen Batteries: Bridging Mechanistic Understanding and Battery Performance. *Energy Environ. Sci.* **2013**, *6*, 750−768.

(2) Franger, S.; Benoit, C.; Saint-Martin, R. The Electrochemical Energy Storage: Contribution of the Rechargeable Lithium-Ion Batteries. *Actual. Chim.* **2008**, 41−44.

(3) Tarascon, J. M.; Armand, M. Issues and Challenges Facing Rechargeable Lithium Batteries. *Nature* **2001**, *414*, 359−367.

(4) Scrosati, B. Recent Advances in Lithium Ion Battery Materials. *Electrochim. Acta* **2000**, *45*, 2461−2466.

(5) Wang, Y. G.; Yi, J.; Xia, Y. Y. Recent Progress in Aqueous Lithium-Ion Batteries. *Adv. Energy Mater.* **2012**, *2*, 830−840.

(6) Nicotera, I.; Oliviero, C.; Henderson, W. A.; Appetecchi, G. B.; Passerini, S. NMR Investigation of Ionic Liquid-Lix Mixtures: Pyrrolidinium Cations and Tfsi- Anions. *J. Phys. Chem. B* **2005**, *109*, 22814−22819.

(7) Borodin, O.; Smith, G. D. Structure and Dynamics of N-Methyl-N-Propylpyrrolidinium Bis(Trifluoromethanesulfonyl)Imide Ionic Liquid from Molecular Dynamics Simulations. *J. Phys. Chem. B* **2006**, *110*, 11481−11490.

(8) Bayley, P. M.; Lane, G. H.; Rocher, N. M.; Clare, B. R.; Best, A. S.; MacFarlane, D. R.; Forsyth, M. Transport Properties of Ionic Liquid Electrolytes with Organic Diluents. *Phys. Chem. Chem. Phys.* **2009**, *11*, 7202−7208.

(9) Raju, S. G.; Balasubramanian, S. Molecular Dynamics Simulation of Model Room Temperature Ionic Liquids with Divalent Anions. *Indian J. Chem., Sect. A: Inorg., Bio-inorg., Phys., Theor. Anal. Chem.* **2010**, *49*, 721−726.

(10) Wang, Y. T.; Voth, G. A. Tail Aggregation and Domain Diffusion in Ionic Liquids. *J. Phys. Chem. B* **2006**, *110*, 18601−18608.

(11) Bayley, P. M.; Best, A. S.; MacFarlane, D. R.; Forsyth, M. The Effect of Coordinating and Non-Coordinating Additives on the Transport Properties in Ionic Liquid Electrolytes for Lithium Batteries. *Phys. Chem. Chem. Phys.* **2011**, *13*, 4632−4640.

(12) Seki, S.; Kobayashi, Y.; Miyashiro, H.; Ohno, Y.; Usami, A.; Mita, Y.; Kihira, N.; Watanabe, M.; Terada, N. Lithium Secondary Batteries Using Modified-Imidazolium Room-Temperature Ionic Liquid. *J. Phys. Chem. B* **2006**, *110*, 10228−10230.

(13) Lane, G. H.; Best, A. S.; MacFarlane, D. R.; Forsyth, M.; Bayley, P. M.; Hollenkamp, A. F. The Electrochemistry of Lithium in Ionic Liquid/Organic Diluent Mixtures. *Electrochim. Acta* **2010**, *55*, 8947−8952.

(14) Hardwick, L. J.; Holzapfel, M.; Wokaun, A.; Novak, P. Raman Study of Lithium Coordination in Emi-Tfsi Additive Systems as Lithium-Ion Battery Ionic Liquid Electrolytes. *J. Raman Spectrosc.* **2007**, *38*, 110−112.

(15) Xu, J. Q.; Yang, J.; NuLi, Y.; Wang, J. L.; Zhang, Z. S. Additive-Containing Ionic Liquid Electrolytes for Secondary Lithium Battery. *J. Power Sources* **2006**, *160*, 621−626.

(16) Choi, J. A.; Eo, S. M.; MacFarlane, D. R.; Forsyth, M.; Cha, E.; Kim, D. W. Effect of Organic Additives on the Cycling Performances of Lithium Metal Polymer Cells. *J. Power Sources* **2008**, *178*, 832−836.

(17) Yamaguchi, T.; Nagao, A.; Matsuoka, T.; Koda, S. A Theoretical Study on the Anomalous Pressure Dependence of the Transport Properties of Ionic Liquids: Comparison Among Lithium Bromide, Silica, and Water. *J. Chem. Phys.* **2003**, *119*, 11306−11317.

(18) Borodin, O.; Smith, G. D.; Henderson, W. Li^+ Cation Environment, Transport, and Mechanical Properties of the Litfsi Doped N-Methyl-N-Alkylpyrrolidinium + Tfsi- Ionic Liquids. *J. Phys. Chem. B* **2006**, *110*, 16879−16886.

(19) Rey-Castro, C.; Tormo, A. L.; Vega, L. F. Effect of the Flexibility and the Anion in the Structural and Transport Properties of Ethyl-Methyl-Imidazolium Ionic Liquids. *Fluid Phase Equilib.* **2007**, *256*, 62−69.

(20) Cadena, C.; Zhao, Q.; Snurr, R. Q.; Maginn, E. J. Molecular Modeling and Experimental Studies of the Thermodynamic and Transport Properties of Pyridinium-Based Ionic Liquids. *J. Phys. Chem. B* **2006**, *110*, 2821−2832.

(21) Koishi, T.; Tamaki, S. A Theory of Transport Properties in Molten Salts. *J. Chem. Phys.* **2005**, 123.

(22) Chang, T. M.; Dang, L. X.; Devanathan, R.; Dupuis, M. Structure and Dynamics of N,N-Diethyl-N-methylammonium Triflate Ionic Liquid, Neat and with Water, from Molecular Dynamics Simulations. *J. Phys. Chem. A* **2010**, *114*, 12764−12774.

(23) Green, M. D.; Choi, J. H.; Winey, K. I.; Long, T. E. Synthesis of Imidazolium-Containing ABA Triblock Copolymers: Role of Charge Placement, Charge Density, and Ionic Liquid Incorporation. *Macromolecules* **2012**, *45*, 4749−4757.

(24) Ditchfield, R.; Hehre, W. J.; Pople, J. A. Self-Consistent Molecular Orbital Methods. 9. Extended Gaussian-Type Basis for Molecular-Orbital Studies of Organic Molecules. *J. Chem. Phys.* **1971**, *54*, 724.

(25) Hehre, W. J.; Ditchfield, R.; Pople, J. A. Self-Consistent Molecular Orbital Methods. 12. Further Extensions of Gaussian-Type Basis Sets for Use in Molecular-Orbital Studies of Organic-Molecules. *J. Chem. Phys.* **1972**, *56*, 2257.

(26) Hariharan, P. C.; Pople, J. A. Influence of Polarization Functions on Molecular-Orbital Hydrogenation Energies. *Theor. Chem. Acc.* **1973**, *28*, 213.

(27) Gordon, M. S. The Isomers of Silacyclopropane. *Chem. Phys. Lett.* **1980**, *76*, 163−168.

(28) Francl, M. M.; Pietro, W. J.; Hehre, W. J.; Binkley, J. S.; Gordon, M. S.; Defrees, D. J.; Pople, J. A. Self-Consistent Molecular-Orbital Methods. 23. A Polarization-Type Basis Set for 2nd-Row Elements. *J. Chem. Phys.* **1982**, *77*, 3654−3665.

(29) Binning, R. C.; Curtiss, L. A. Compact Contracted Basis-Sets for 3rd-Row Atoms - Ga-Kr. *J. Comput. Chem.* **1990**, *11*, 1206−1216.

(30) Blaudeau, J. P.; McGrath, M. P.; Curtiss, L. A.; Radom, L. Extension of Gaussian-2 (G2) Theory to Molecules Containing Third-Row Atoms K and Ca. *J. Chem. Phys.* **1997**, *107*, 5016−5021.

(31) Rassolov, V. A.; Pople, J. A.; Ratner, M. A.; Windus, T. L. 6-31G* Basis Set for Atoms K Through Zn. *J. Chem. Phys.* **1998**, *109*, 1223−1229.

(32) Plimpton, S. Fast Parallel Algorithms for Short-Range Molecular-Dynamics. *J. Comput. Phys.* **1995**, *117*, 1−19.

(33) Watkins, E. K.; Jorgensen, W. L. Perfluoroalkanes: Conformational Analysis and Liquid-State Properties from Ab Initio and Monte Carlo Calculations. *J. Phys. Chem. A* **2001**, *105*, 4118−4125.

(34) Martyna, G. J.; Tobias, D. J.; Klein, M. L. Constant-Pressure Molecular-Dynamics Algorithms. *J. Chem. Phys.* **1994**, *101*, 4177−4189.

(35) Parrinello, M.; Rahman, A. Polymorphic Transitions in Single-Crystals - A New Molecular-Dynamics Method. *J. Appl. Phys.* **1981**, *52*, 7182−7190.

(36) Tuckerman, M. E.; Alejandre, J.; Lopez-Rendon, R.; Jochim, A. L.; Martyna, G. J. A Liouville-Operator Derived. Measure-Preserving Integrator for Molecular Dynamics Simulations in the Isothermal-Isobaric Ensemble. *J. Phys. A: Math. Gen.* **2006**, *39*, 5629−5651.
(37) Shinoda, W.; Shiga, M.; Mikami, M. Rapid Estimation of Elastic Constants by Molecular Dynamics Simulation under Constant Stress. *Phys. Rev. B* **2004**, *69*, 8.
(38) Nose, S. A Molecular Dynamics Method For Simulations in the Canonical Ensemble. *Mol. Phys.* **2002**, *100*, 191−198.
(39) Nose, S. An Extension of the Canonical Ensemble Molecular-Dynamics Method. *Mol. Phys.* **1986**, *57*, 187−191.
(40) Nose, S. A Unified Formulation of the Constant Temperature Molecular-Dynamics Methods. *J. Chem. Phys.* **1984**, *81*, 511−519.
(41) Nose, S.; Klein, M. L. Constant Pressure Molecular-Dynamics for Molecular-Systems. *Mol. Phys.* **1983**, *50*, 1055−1076.
(42) Hoover, W. G. Canonical Dynamics - Equilibrium Phase-Space Distributions. *Phys. Rev. A* **1985**, *31*, 1695−1697.
(43) Darden, T.; York, D.; Pedersen, L. Particle Mesh Ewald - An N.Log(N) Method for Ewald Sums in Large Systems. *J. Chem. Phys.* **1993**, *98*, 10089−10092.
(44) Toukmaji, A.; Sagui, C.; Board, J.; Darden, T. Efficient Particle-Mesh Ewald Based Approach to Fixed and Induced Dipolar Interactions. *J. Chem. Phys.* **2000**, *113*, 10913−10927.
(45) Eastwood, J. W.; Hockney, R. W.; Lawrence, D. N. P3M3DP - The 3-Dimensional Periodic Particle-Particle-Particle-Mesh Program. *Comput. Phys. Commun.* **1980**, *19*, 215−261.
(46) Kolafa, J.; Perram, J. W. Cutoff Errors in the Ewald Summation Formulas For Point-Charge Systems. *Mol. Simul.* **1992**, *9*, 351−368.
(47) Petersen, H. G. Accuracy and Efficiency of the Particle Mesh Ewald Method. *J. Chem. Phys.* **1995**, *103*, 3668−3679.
(48) Wang, Z. W.; Holm, C. Estimate of the Cutoff Errors in the Ewald Summation for Dipolar Systems. *J. Chem. Phys.* **2001**, *115*, 6351−6359.
(49) Pollock, E. L.; Glosli, J. Comments on P(3)M, FMM, and the Ewald Method for Large Periodic Coulombic Systems. *Comput. Phys. Commun.* **1996**, *95*, 93−110.
(50) Isele-Holder, R. E.; Mitchell, W.; Ismail, A. E. Development and Application of a Particle-Particle Particle-Mesh Ewald Method for Dispersion Interactions. *J. Chem. Phys.* **2012**, *137*, 13.
(51) Hardy, D. J.; Stone, J. E.; Schulten, K. Multilevel Summation of Electrostatic Potentials Using Graphics Processing Units. *Parallel Comput.* **2009**, *35*, 164−177.
(52) Allen, M. P.; Tildesley, D. J. *Computer Simulation of Liquids*. Oxford University Press: New York, 1987.
(53) Frenkel, D.; Smit, B. *Understanding Molecular Simulation: From Algorithms to Applications*, 2nd ed.; Academic Press: New York, 2001.
(54) Wu, T. Y.; Hao, L.; Chen, P. R.; Liao, J. W. Ionic Conductivity and Transporting Properties in LiTFSI-Doped Bis-(trifluoromethanesulfonyl)imide-Based Ionic Liquid Electrolyte. *Int. J. Electrochem. Sci.* **2013**, *8*, 2606−2624.
(55) Bayley, P. M.; Best, A. S.; MacFarlane, D. R.; Forsyth, M. Transport Properties and Phase Behaviour in Binary and Ternary Ionic Liquid Electrolyte Systems of Interest in Lithium Batteries. *ChemPhysChem* **2011**, *12*, 823−827.